IOP Conference Series:
Materials Science and
Engineering

PAPER • **OPEN ACCESS**

Thermal Spraying of CuAlFe Powder on Cu_5Sn Alloy

To cite this article: I C Roata *et al* 2017 *IOP Conf. Ser.: Mater. Sci. Eng.* **209** 012042

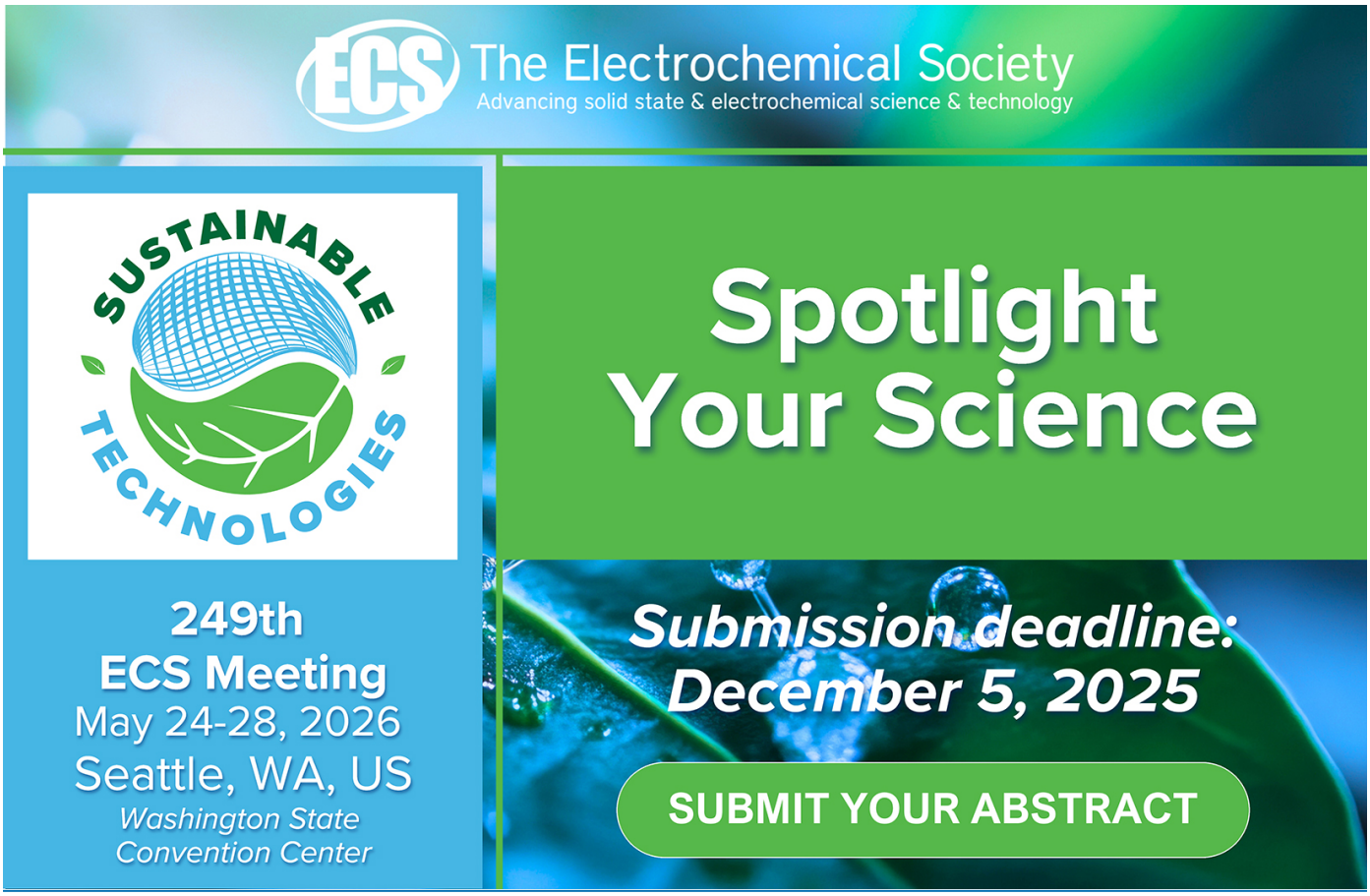

IOP Conf. Series: Materials Science and Engineering **209** (2017) 012042 doi:10.1088/1757-899X/209/1/012042

Thermal Spraying of CuAlFe Powder on Cu_5Sn Alloy

I C Roata*, A Pascu, C Croitoru[1], E M Stanciu[1] and M A Pop[2]
[1]Materials Engineering and Welding Department, Transilvania University of Brasov, Romania
[2]Materials Science Department, Transilvania University of Brasov, Romania

E-mail: ionut.roata@unitbv.ro

Abstract. To improve the corrosion and wear resistance of copper and its alloys, flame spraying has been employed to obtain a relatively homogenous Cu/Al/Fe-based coating. To minimize the defects that usually occur by using this method, a post-coating annealing step has been employed, by using concentrated solar energy as means of thermal surface treatment. Scanning electron micrographs have indicated a reduction in the cracks/pores density and accelerated corrosion testing have indicated a higher performance of the solar-annealed sample, in comparison with the initial reference material. The coating approach mentioned in this paper could be successfully applied to restore several worn tools and instruments, and could also be of use in the renewable energy field (IR-absorbent coatings) or in advanced oxidation processes, such as photocatalysis.

1. Introduction

Thermal spraying comprises in a group of processes through which various metallic or non-metallic feedstock materials (in powder, rod, or wire form) are brought in melted or semi-melted state using a heat source, after which they are accelerated and propelled on a substrate. The propelling of the coating material is responsible for spreading and bonding to the desired substrate [1].

Among the conventional thermal spraying methods, flame spraying is by far the most economically efficient approach to deposit a large variety of coatings, using as fuel sources hydrogen or several saturated and unsaturated hydrocarbons (propane, acetylene and so forth) which in reaction with a comburant (air, oxygen) produce an appropriate heat source, used for melting or plastic state achieving, as well as in creating a compressed gas steam that atomizes the molten particles and accelerates them onto the substrate [2-4].

Usually, all the thermal processes generate coatings with lamellar grain structure, because of rapid solidification of small globule particles, which are flattened by striking the cold substrate surface at high velocities. The thermal sprayed coatings usually present a large density of defects (cracks, pores, foreign particles inclusions), coating material and substrate oxidation due to the high temperatures which generates delamination, de-bonding, and therefore poor mechanical and corrosion-resistance performance. Currently, approaches designed to mitigate these shortcomings are limited to applying a post-deposition thermal heat treatment that reduces the number of defects through splats re-melting. This has detrimental effects on coating hardness and bonding to the substrate [5-10].

In this study, the flame spraying method has been used to obtain a cooper-aluminium coating deposited on a Cu_5Sn alloy, with potential use in manufacturing of electrical contacts, in the renewable energy field (IR absorbent coatings) or as photocatalysis substrate. To obtain an improved homogeneity of the coating, both in compositional as well as in morphological terms, a concentrated

solar post-deposition thermal treatment has been employed. The benefit of using solar energy for thermal treatment resides in its accessibility, economic effectiveness and ”green” character, thus avoiding the use of other usual and more environmentally-demanding heating processes, such as oven heat treatments, induction heating or molten salts thermal treatment [11].

2. Experimental

2.1. Materials

Rectangular samples (l=20 mm, L=20 mm, h=25 mm) of Cu5Sn alloy have been used as substrate for the flame spraying process, in conjunction with a Cu-Al-Fe powder, acquired from Castolin Eutectic, Germany. The elemental composition of the powder is presented in table 1.

Table 1. The chemical composition of Cu-Al-Fe coating powder.

Element	Composition (wt. %)
Cu	Balance
Al	8.5 – 10.75
Fe	0.5 - 2

The powder presents a core-shell type of morphology, with a copper core and an aluminum-iron coating. This configuration has been proven to aid interphase elemental diffusion and thus the formation of hard phases.

2.2. Methods

2.2.1. Thermal spraying and solar heat treatment of obtained coatings. The coatings obtaining has been realised in two steps. Firstly, the powder has been applied on the copper substrate by using the flame spraying method and secondly, a surface thermal treatment has been applied to improve splat adhesion, minimize the number of defects and to promote the formation of hard-phases in the material and refinement of the microstructure.

The coating was obtained by using a CastoDyn DS8000 flame and powder metallizing unit. C_2H_2 (0.7 bar pressure) has been employed as carburant gas and oxygen (4 bar pressure) as comburant, by utilizing a spraying distance of 150 mm, as shown in table 2. This distance has been selected by taking into consideration that at spraying distances lower than 100 mm, superficial layer exfoliation associated with material oxidation takes place because of overheating, and at large spraying distances (> 200 mm) an enhanced level/degree of porosity and poor adhesion could occur owing to the embedding a high quantity of cold particles in the coated material.

Because thermally sprayed coatings are inhomogeneous, all prepared samples have been thermally treated at the surface by solar heat fusion. Solar heat treatment has been performed with the help of a SF5 furnace (1 – 5 kW) having a 2.5 cm solar spot diameter, at the Plataforma Solar de Almería (PSA), a dependency of the Centro de Investigaciones Energéticas, Medioambientales y Tecnológicas (CIEMAT), the biggest concentrating solar technology inquiry, improvement, and test centre in Europe [11].

The solar thermal treatment plant scheme is described in figure 1.

A thorough control of solar thermal treatment has been carried out by using a thermocouple inserted in a drilled hole in the middle of the samples. Several samples were fully melted to define the operational temperature domain (maximum of 970°C).

Thermal treatment of the samples has been achieved in four distinct steps, illustrated in figure 2: I) sample preheating at the temperature of 600ºC (T1); II) maintaining the preheating temperature for 5 min (T_1-T_2); III) heating at 950ºC with 50ºC/min (T3), followed by IV) cooling the samples at room temperature (T4).

Table 2. Operational parameters of the thermal spraying process.

Parameters	Sample 1 S1	Sample 2 S2
Thermal spraying distance	150 mm	150 mm
Powder feed rate	38 g/min	38 g/min
Preheating	120 ºC	120 ºC
Oxygen pressure	4 bar	4 bar
Acetylene pressure	0.7 bar	0.7 bar

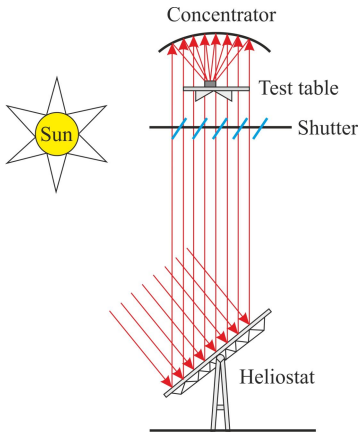

Figure 1. Functional diagram of the SF05 solar furnace.

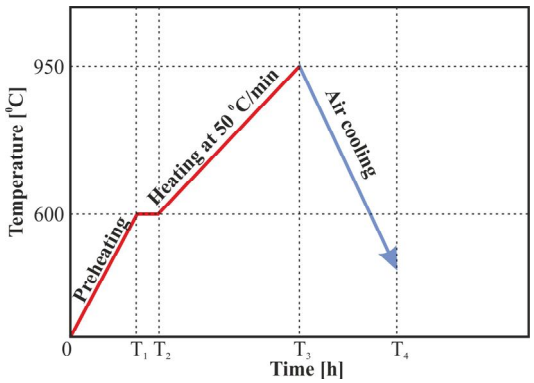

Figure 2. Solar heat treatment diagram.

2.2.2. Scanning electron microscopy (SEM) and microhardness tests The cross-section electron micrographs of the flame-sprayed samples have been achieved by utilizing a scanning electron microscope (SEM) Quanta 3D 200i model at various magnifications, mentioned on each micrograph. The elemental distribution of Cu, Al and Fe within the coating as well as in the boundary region was outlined with the help of energy-dispersive X-ray spectroscopy (EDS).

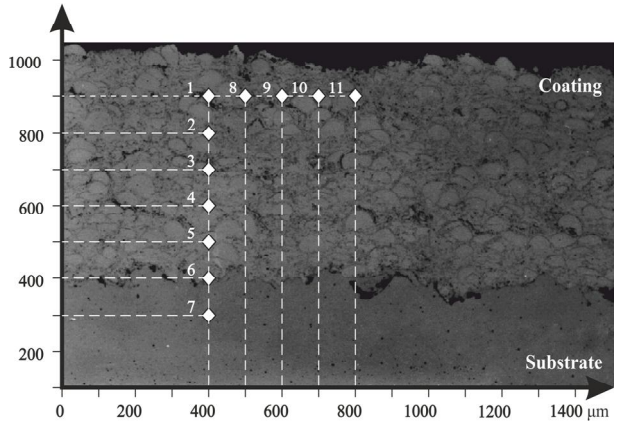

Figure 3. Positioning of microhardness indentations.

The microhardness tests were obtained on a FM 700 durometer, by employing 11 tests of HV_{01} in distinct zones, both on the coating as well as in the substrate material, as indicated in figure 3. A force of 1 N with a 15 seconds penetrator holding time has been used.

2.2.3. Corrosion testing. For the accelerated corrosion tests, an aqueous solution with global concentrations of 25% wt. NaCl; 1% wt. HNO_3 and 3% wt. H_2O_2 has been used. This solution is especially used in conjunction with aluminum and copper alloys to test for inter-grain corrosion or surface pitting. The samples have been weighed initially (m_0) and then immersed in 10 ml of the corrosion test solution for 1 hour, with the coating facing downward. The volume of the corrosion solution and the diameter of the recipients in which the corrosion testing has been performed were chosen such as only the coating is in contact with the corrosive environment. After 1 hour, the samples have been washed several times with distilled water, dried and reweighted (m_1). The relative mass loss due to corrosion (Δm_{corr}) has been determined with eq. 1:

$$\Delta m_{corr} = \frac{m_0 - m_1}{m_0} \cdot 100(\%) \quad (1)$$

Copper ions leaching from the coating to the aqueous environment has been visually assessed.

3. Results and discussion

3.1. Structure of the Cu-Al-Fe coatings

Figure 4 (S1) presents the cross-section electron micrographs of the Cu-Al-Fe intermetallic coatings before heat treatment and (S2) after heat treatment at 950ºC.

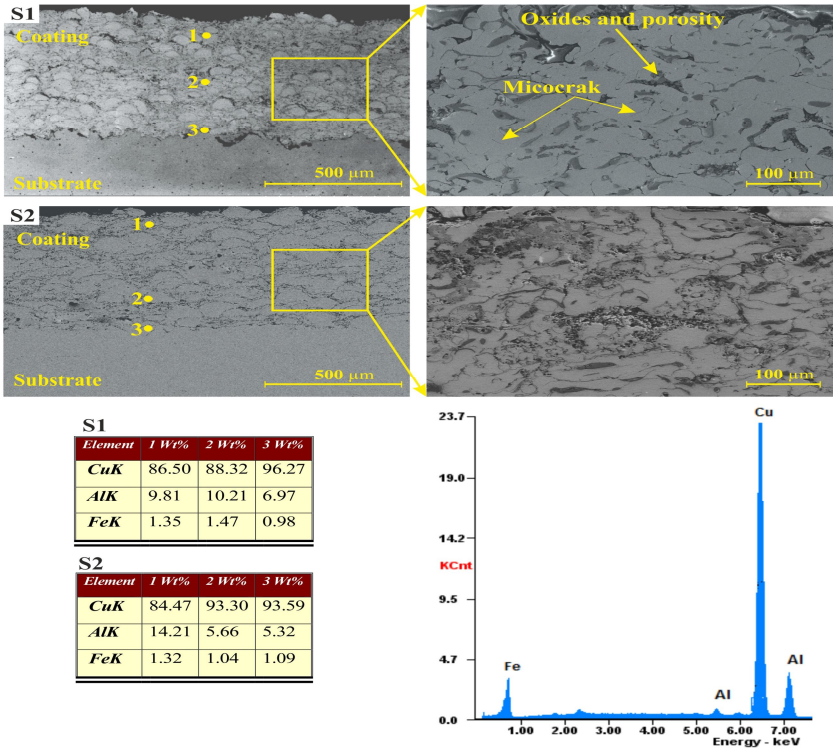

Figure 4. Cross-sectional SEM micrographs of S1 (initial sample) and S2 (heat treated at 950ºC).

The S1 sample presents a typical lamellar (multi-layered) aspect and in some regions, partly unmelted splats could be evidenced as result of the thermal spraying process. Both dense splat and close-grained structures can be observed in the SEM micrographs as outcome of consecutive coating processes and resolidification of molten or semi-molten droplets.
Moreover, the interface with the substrate displays pores, partial melting, and high density of oxides.

An improvement in the coating bonding to the substrate has been achieved by employing solar energy, as it could be observed from Figure 4. A clear reduction in the cracks and pores density of the coating has been obtained, which aids in an improved wear and corrosion resistance performance of the material. The chemical composition variation along the coating (from the top to the substrate) indicates an improved inter-mixing of elements in the case of S2 sample, possibly with the formation of different hardphases, such as $CuAl_2$ mentioned also in other research performed on the Cu-Al coating system [12-14], that may be responsible for the improved corrosion resistance of the material.

3.2. Micro-hardness of the coatings

The minimum and maximum micro-hardness values of the Cu-Al-Fe coating marked along the cross-section of the coating are 149.78 and 158.09 HV_{01}. Along the coating a ± 1 % variation occurred, indicating a relatively high compositional homogeneity of the coating material.

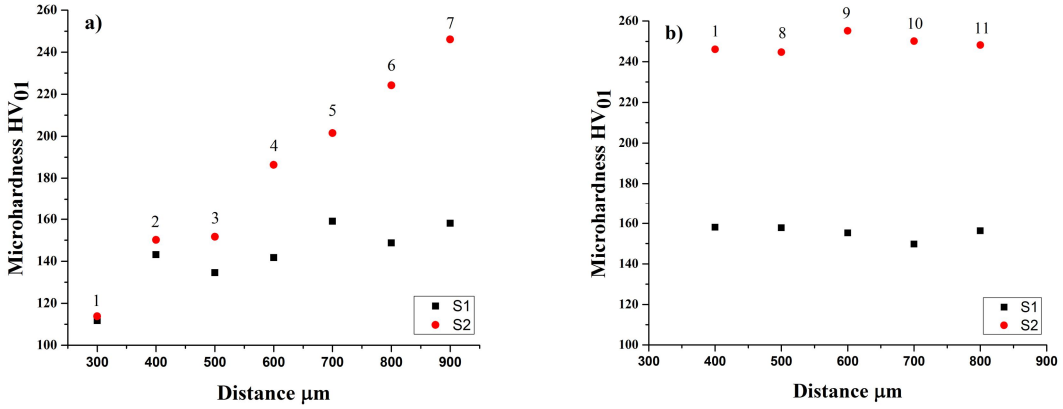

Figure 5 The influence of the temperature on the hardness values at different distances measured from the coating to the substrate (a) and the influence of temperature on the hardness along the coating (b).

The usage of solar heat treatment leads to a coating hardness increase from 158.09 $HV_{0.1}$ (S1) to 255.18 (S2) (figure 5). Figure 5b reveals that the micro-hardness longitudinally measured on the cross section for sample S2 is around 249 HV_{01} compared with 155 HV_{01} in the case of reference sample S1. This hardness increase in the solar annealed sample could be related to hardphases formation and subsequently could be linked with an improved corrosion performance.

3.3. Corrosion performance

Figure 6 illustrates the surface morphology before and after accelerated corrosion testing of the reference and solar-annealed samples.

An advanced corrosion of both aluminium and copper has been registered in the case of the non-annealed S1 sample, also by evidencing the colour differences of the solutions after the corrosion experiments. The mass loss value for S1 was 0.4996 %, in contrast with only 0.1919% for S2, indicating approximatively a threefold increase in the corrosion resistance after solar annealing.

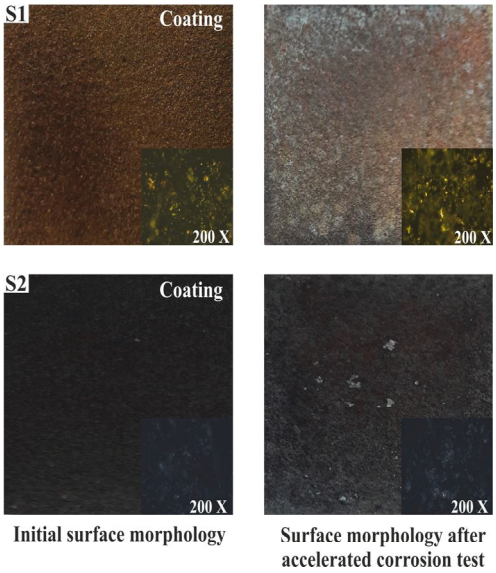

Figure 6. Corrosion testing of the flame-sprayed samples.

4. Conclusion

Ternary copper-aluminum-iron composite coatings have been obtained through flame spraying of a special core/shell powder. The characteristic defects, such as pores and cracks density has been reduced through applying a short post-deposition concentrated solar energy thermal treatment. Through this treatment, intermetallic hard-phases are formed which contribute to microhardness and corrosion resistance increase.

References

[1] Zhang P, Lau YY, 2010 *Journal of Applied Physics* **108** 44914
[2] Rahmana A, Jayaganthana R, Prakasha S, 2009 *J Alloys Compd.* **478** 472
[3] Hefei Li, Shufeng Tao, Zhaohui Zhou, Lidong Sun, A. Hesnawi, Shengkai Gong, 2007 *Surf. Coat. Techno* **201** 6589
[4] Mulero M.A., Zapata J, Vilar R, Martinez V, Gadow R, 2015 *Surf. Coat. Techno.* **278** 1
[5] Davis J.R. et al. 2004 *Handbook of Thermal Spray Technology,* ASM Int. 3-54
[6] Picas J.A, Forn A, Rilla R, Martin E, 2005 *Surf. Coat. Technol.* **200** 1178
[7] Fanicchia F, Axinte D.A, Kell J et al., 2017 *Surf. Coat. Technol.* **315** 546
[8] Houdková Š, Smazalová E, Vostřák M, Schuber J, 2014 *Surface & Coatings Technology* **253** 14
[9] Suutala J, Tuominen J, Vuoristo P, 2006 *Surface & Coatings Technology* **201** 1981
[10] Li C.J, Yang G.J, 2013 *Journal of Refractory Metals and Hard Materials* **39** 2
[11] Rodríguez J, Cañadas I, Zarza E, 2014 *Energy Procedia,* **49** 1511
[12] Yang J, Zhang Y, Zhao X, An Y, Zhou H, Hou J.G, 2015 *Tribology International* **90** 96.
[13] Zhao X, An Y, Hou G, Zhou H, Chen J, 2016 *Tribology International* **101** 255
[14] Zhang J, Wang B, Chen G, Wang R, Miao C, Zheng Z, Tang W, 2016 *Trans. Nonferrous Met. Soc. China* **26** 3283

Acknowledgements

Financial support by the Access to Research Infrastructures activity in the 7th Framework Programme of the EU (SFERA 2 Grant Agreement n. 312643) is gratefully acknowledged. The ICIR Euroinvent 2017 Conference mobility expenses have been supported by a grant of the Romanian National Authority for Scientific Research and Innovation, CNCS - UEFISCDI, project number PN-II-RU-TE-2014-4-0173.